



This is a repository copy of *On the correct choice of equivalent circuit for fitting bulk impedance data of ionic/electronic conductors*.

White Rose Research Online URL for this paper:
<http://eprints.whiterose.ac.uk/99068/>

Version: Accepted Version

Article:

West, A.R. orcid.org/0000-0002-5492-2102, Hernández, M.A. and Masó, N. (2016) On the correct choice of equivalent circuit for fitting bulk impedance data of ionic/electronic conductors. *Applied Physics Letters*, 108 (15). 152901. ISSN 0003-6951

<https://doi.org/10.1063/1.4946008>

Reuse

Unless indicated otherwise, fulltext items are protected by copyright with all rights reserved. The copyright exception in section 29 of the Copyright, Designs and Patents Act 1988 allows the making of a single copy solely for the purpose of non-commercial research or private study within the limits of fair dealing. The publisher or other rights-holder may allow further reproduction and re-use of this version - refer to the White Rose Research Online record for this item. Where records identify the publisher as the copyright holder, users can verify any specific terms of use on the publisher's website.

Takedown

If you consider content in White Rose Research Online to be in breach of UK law, please notify us by emailing eprints@whiterose.ac.uk including the URL of the record and the reason for the withdrawal request.



eprints@whiterose.ac.uk
<https://eprints.whiterose.ac.uk/>

ON THE CORRECT CHOICE OF EQUIVALENT CIRCUIT FOR FITTING BULK IMPEDANCE DATA OF IONIC/ELECTRONIC CONDUCTORS

Miguel A. Hernández^a, Nahum Masó^{a,b} and Anthony R. West^a

^aDepartment of Materials Science and Engineering, The University of Sheffield, Mappin St,
Sheffield S1 3JD, U.K

^bCurrent address: CNRS, Institut Carnot CIRIMAT, Université Paul-Sabatier, 118 route de
Narbonne, 31062 Toulouse Cedex 9, France.

Abstract

Bulk conductivity data of ionically- and electronically-conducting solid electrolytes and electronic ceramics invariably show a frequency dependence that cannot be modelled by a single-valued resistor. To model this, common practice is to add a constant phase element, CPE, in parallel with the bulk resistance. To fit experimental data on a wide variety of materials, however, it is also essential to include the limiting, high frequency permittivity of the material in the equivalent circuit. Failure to do so can lead to incorrect values for the sample resistance and CPE parameters and to an inappropriate circuit for materials that are electrically heterogeneous

In the analysis and interpretation of impedance data, it is always essential to represent the data by an equivalent circuit in order to have correct equations to determine values for the component resistance, R , and capacitance, C , parameters. Selection of the most appropriate equivalent circuit is not always straightforward, especially for heterogeneous ceramics whose grains and grain boundaries may be distinct electrically and in many cases, where electrode-sample contact impedances are also present. In this communication, we do not discuss the strategies that may be adopted to deduce the correct equivalent circuit for heterogeneous materials or systems; these have been covered elsewhere [1] Instead, this paper focuses on one component, the limiting, high frequency bulk response, both for its fundamental importance to materials characterisation but

also, for its necessary inclusion to obtain accurate fitting data on other circuit elements. We illustrate this with two examples, a single crystal ferroelectric, BaTi_2O_5 , which is also a modest semiconductor, and yttria-stabilised zirconia, YSZ, ceramic, the well-known oxide ion conductor.

Figure 1 shows typical impedance data obtained on heating a single crystal of BaTi_2O_5 , BT_2 , prepared and characterised as described in [2], as it changes from an insulating state at 275 °C to semiconducting at 630 °C. At low temperatures, the impedance complex plane plot, Z^* , (a), shows a straight line, nearly parallel to Z'' which passes through the origin; the spectroscopic plot of the real part of the admittance, $\log Y'$ vs $\log f$, shows essentially noisy data (b) since the sample impedance falls outside the measuring range of the instrumentation. However, the spectroscopic plot of the real part of the capacitance, $\log C'$ vs $\log f$, shows a frequency-independent plateau (c) at higher frequencies with associated capacitance, $\sim 6 \text{ pFcm}^{-1}$. This is assigned to the bulk permittivity of the sample, with a value of ~ 70 , calculated from the formula $\epsilon = C / \epsilon_0$ of in which ϵ_0 is the permittivity of free space, 8.854 Fcm^{-1} and C has been corrected for both the geometry of the sample and the stray capacitance of the empty sample holder.

At intermediate temperatures, Z^* shows the high-frequency wing of the bulk semicircle (d) and $\log Y'$ vs $\log f$ shows a frequency-dependent power law behaviour (e) characteristic of Jonscher's Universal Dielectric Response, UDR [3-5]. The $\log C'$ vs $\log f$ plot shows a plateau at high frequency that corresponds to the bulk capacitance and frequency-dependent behaviour at low frequency associated with the UDR (f).

At high temperatures, Z^* shows the bulk semicircle (g); $\log Y'$ vs $\log f$ shows frequency-dependent UDR at high frequency and a plateau at low frequency associated with the *dc* conductivity (h); $\log C'$ vs $\log f$ continues to show a plateau at high frequency and frequency-dependent UDR at low frequency (i). A similar evolution is observed for a polycrystalline sample of 8 mole% Y-stabilised ZrO_2 , YSZ, prepared and characterised as described in [6] (not shown).

Widespread practice for modelling impedance data uses the Z^* plot to present the data and a parallel combination of an R and a constant phase element, CPE or CPQ [$Y_{\text{CPE}}^* = Y_0(j\omega)^n$; $Y_{\text{CPQ}}^* = (Y_0 j\omega)^n$], **Figure 2(a)**, to fit the bulk semicircle [7]. Whilst in certain cases this may give a good fit to Z^* data presented on the usual linear scales, as also shown here for fits to experimental data of BT₂ and YSZ in **Figures 3,4(a)**, the fit quality is seen to be very much worse when the data are presented in other formalisms, such as Z' , Y' and C' against f , all on logarithmic scales, **Figures 3,4(b-d)**; values of fit parameters, R, C, Y_0 , and n are summarised in **Table I**.

Visually, the Z^* plots on linear scales are modelled reasonably well (a) and, consequently, values of R and the pseudocapacitance C associated with the CPE for the angular frequency, ω , at the maximum of the semicircle are obtained from the fitting (R) and calculated by $C = (Y_0 R)^{1/n} R^{-1}$, respectively. However, on converting Z^* to Y' and C' using $M^* = (\epsilon^*)^{-1} = j\omega C_0 Z^* = j\omega C_0 (Y^*)^{-1}$ [8], and plotting the data spectroscopically on logarithmic scales, the fit is poor **Figures 3(b-d)** for Z' and Y' at high frequency and for C' at all frequencies. This illustrates the value of presentation and analysis of the same data in alternative formalisms, which have different in-built weightings, as an exceptionally useful way to assess visually the fit quality.

An alternative strategy, which has been little acknowledged but is based on the fundamental need to include in the circuit the limiting, frequency-independent bulk permittivity of the sample, often referred to as ϵ_{∞} , is to fit the bulk semicircle using a parallel combination of an R, CPE, and C [1,3,6,9], as shown in **Figure 2(b)**. Fits to experimental data of BT₂ and YSZ and values of the fit parameters are shown in **Figures 3,4(e-h)** and **Table I**, respectively. The key difference is that whereas circuit (b) also fits the bulk response reasonably well in the Z^* plot with data presented on linear scales **Figures 3,4(e)**, it also fits well the alternative Z' , Y' , C' spectroscopic formats which, on logarithmic scales, give equal weighting to all data points over the entire frequency range.

We now comment on the reasons why these two alternative circuits may give significantly different fits to experimental data. In addition to the *dc* sample resistance, R, both circuits contain a constant phase element, CPE, whose admittance takes the form:

$$Y_{\text{CPE}}^* = Y_0(j\omega)^n = Y_0\omega^n[\cos(n\pi/2) + j\sin(n\pi/2)] = A\omega^n + jB\omega^n \quad (1)$$

where ω is the angular frequency $2\pi f$, $j=\sqrt{-1}$ and A and B are inter-related by the Kramers-Kronig relationship [10], $B/A = \tan(n\pi/2)$: $0 < n < 1$. However, in addition to R which represents the low frequency limiting resistance, circuit **Figure 2(b)** also contains capacitance, C that represents the limiting high frequency permittivity of the material. Thus, Y' for both circuits is the same and is given by:

$$Y' = R^{-1} + Y_0\omega^n \cos(n\pi/2) = R^{-1} + A\omega^n \quad (2)$$

whereas C' is different for the two circuits and is given by:

$$\text{circuit a: } C' = Y_0\omega^{n-1} \sin(n\pi/2) = B\omega^{n-1} \quad (3)$$

$$\text{circuit b: } C' = C + Y_0\omega^{n-1} \sin(n\pi/n) = C + B\omega^{n-1} \quad (4)$$

Consequently, in the presentation of $\log C'$ vs $\log f$, both circuits show a low frequency power law response of gradient $(n-1)$, but only circuit **(b)** shows a high frequency plateau that represents the limiting high frequency permittivity, ϵ_{∞} . In cases where experimental data extend to frequencies that are high enough to see a reasonable contribution from ϵ_{∞} , such as shown here for both BT_2 and YSZ, then circuit **(a)** is constrained to give a linear fit to data that are clearly non-linear. The resulting value of the CPE gradient is then in error, as shown also by the lack of agreement with high frequency, Y' data, **Figures 3,4(c)**. In cases where experimental C' data contain little or no contribution from ϵ_{∞} , a linear power law response of C' may be expected and the simplified circuit **(a)** may then fit the data. However, as shown, it cannot be assumed that this is the case and a more complete analysis than obtained by inspection of data in the Z^* representation alone is required.

Fitting of high frequency data, such as these for the BT_2 and YSZ samples, is a first step in a full analysis of the impedance of the ceramic, which at lower frequencies / higher temperatures,

contains contributions arising from dipole reorientation, grain boundaries and sample-electrode interfaces as described elsewhere [1,2,11].

Capacitance data of the kind shown in **Figures 3,4(d,h)**, with a frequency-independent, high frequency plateau have been observed in a wide range of ionically– and electronically– conducting materials, including $\text{La}_{0.80}\text{Sr}_{0.20}\text{Ga}_{0.83}\text{Mg}_{0.17}\text{O}_{2.82}$, $\text{CaCu}_3\text{Ti}_4\text{O}_{12}$, β -alumina, $\text{Ag}_6\text{I}_4\text{WO}_4$, $\text{Bi}_2\text{Mg}_x\text{V}_{1-x}\text{O}_{5.5-1.5x-\delta}$, $\text{Bi}_{12}\text{TiO}_{20}$, BiFeO_3 and AgI [1,9,12–17]. The power law dispersion in C' at lower frequencies and Y' at higher frequencies is a manifestation of Jonscher's Universal Dielectric Response and can be represented by a CPE. The CPE contributes to impedance data over an infinite range of frequencies unless this is terminated at high frequencies by the presence of the parallel capacitance, C , and at low frequencies by the parallel resistance, R . There is, of course, no question over the need for R in circuits of materials that are *dc* conductors, but less recognition of the need for C , as shown by the widespread use of circuits such as **Figure 2(a)**, even though the concept of a limiting high frequency bulk permittivity is extremely well established for many materials.

The principal conclusion of this communication is, therefore, that C must always be included in the equivalent circuit. If it is not, then the fitted CPE values may be in error which in turn, may have consequences for the value of R that is extracted, Table 1 and for fitting data to more complex circuits such as those containing grain boundary or dipolar impedances

References

- [1] E. J. Abram, D. C. Sinclair, and A. R. West, "A Strategy for Analysis and Modelling of Impedance Spectroscopy Data of Electroceramics: Doped Lanthanum Gallate," *J. Electroceram.* **10** [3] 165–177 (2003).
- [2] N. Masó, X.-Y. Yue, T. Goto, and A. R. West, "Frequency-dependent electrical properties of ferroelectric BaTi_2O_5 single crystal," *J. Appl. Phys.* **109** [2] 024107 8pp. (2011).
- [3] A. K. Jonscher, "The 'universal' dielectric response," *Nature* **267** 673 - 679 (1977).
- [4] A. K. Jonscher, "Dielectric Relaxation in Solids", Chelsea Dielectric Press, London, 1983.

- [5] A. K. Jonscher, "Universal Relaxation Law", Chelsea Dielectric Press, London, 1996.
- [6] N. Masó, and A. R. West, "Electronic conductivity in yttria-stabilized zirconia under a small *dc* bias," *Chem. Mater.* **27** [5] 1552–1558 (2015).
- [7] Bruno Yeum, "Tech note 24 – Pseudocapacitance associated with CPE"
- [8] I. M. Hodge, M. D. Ingram and A. R. West, "Impedance and modulus spectroscopy of polycrystalline solid electrolytes", *J. Electroanal. Chem.*, **74** 125-143 (1976)
- [9] P. Lunkenheimer, R. Fichtl, S. G. Ebbinghaus, and A. Loidl, "Non-intrinsic origin of the colossal dielectric constants in $\text{CaCu}_3\text{Ti}_4\text{O}_{12}$," *Phys. Rev. B* **70** [17] 172102 4pp. (2004).
- [10] I. D. Raistrick, C. Ho, and R. A. Huggins, "Closure to 'Discussion of ionic conductivity of some lithium silicates and aluminosilicates'," *J. Electrochem. Soc.* **124** [6] 872–873 (1977)
- [11] M. A. Hernandez and A. R. West, "Dipolar relaxation and impedance of an yttria-stabilised zirconia ceramic electrolyte", *J. Materials Chemistry A*, **[4]** 1298-1305 (2016)
- [12] P. G. Bruce, A. R. West and D. P. Almond, "A new analysis of *ac* conductivity data in single crystal β -alumina," *Solid State Ionics* **7** [1] 57–60 (1982).
- [13] A. Magistris and G. Chiodelli, "*ac* conductivity and dielectric response of the ionic conductor $\text{Ag}_6\text{I}_4\text{WO}_4$," *Electrochim. Acta* **26** [9] 1241–1246 (1981).
- [14] J. R. Dygas, M. Malys, F. Krok, W. Wrobel, A. Kozanecka, and I. Abrahams, "Polycrystalline BIMGVOX.13 studied by impedance spectroscopy," *Solid State Ionics* **176** [25–28] 2085–2093 (2005).
- [15] S. Lanfredi, J. F. Carvalho and A. C. Hernandez, "Electric and dielectric properties of $\text{Bi}_{12}\text{TiO}_{20}$ single crystals," *J. Appl. Phys.* **88** [1], 283–287 (2000).
- [16] A. Perejón, N. Masó, A. R. West, P. E. Sánchez-Jiménez, R. Poyato, J. M. Criado, and L. A. Pérez-Maqueda, "Electrical properties of stoichiometric BiFeO_3 prepared by mechanosynthesis with either conventional or spark plasma sintering", *J. Am. Ceram. Soc.* **96** [4] 1220–1227 (2013).
- [17] S.-H. Moon, D.-C. Cho, D. T. Nguyen, E.-C. Shin, J.-S. Lee, "A comprehensive treatment of universal dispersive frequency responses in solid electrolytes by immittance spectroscopy: low temperature AgI case," *J. Solid State Electrochem.* **19** [8] 2457–2464 (2015).

Table I. R, C, n and Y_0 data for circuits (a) and (b). For circuit (a), C represents the calculated pseudocapacitance.

	Circuit	R (kΩ cm)	n	Y_0 (pS cm⁻¹ Hz⁻ⁿ)	C (pF cm⁻¹)
BT₂	a	227(1)	0.942(3)	228(7)	124(4)
	b	239(1)	0.564(9)	290(30)	100.4(2)
YSZ	a	1406(7)	0.894(3)	29(1)	8.7(3)
	b	1484(7)	0.605(9)	320(30)	5.58(3)

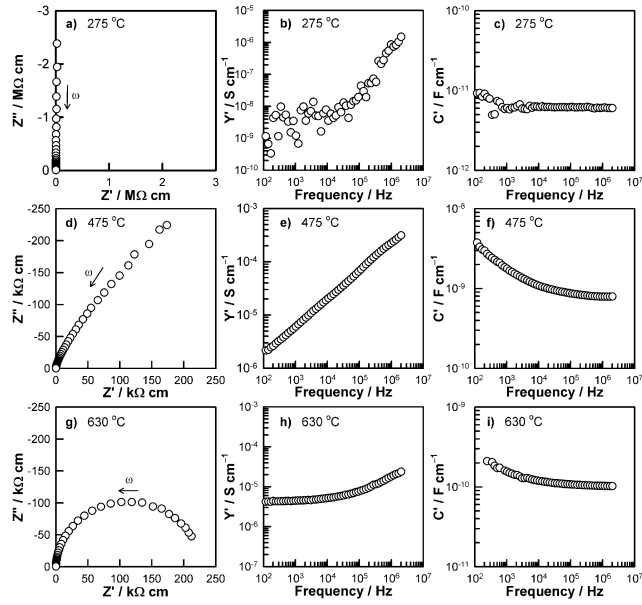


Figure 1. BT₂: impedance complex plane plots (a,d,g) and spectroscopic plots of Y' (b,e,h) and C' (c,f,i).

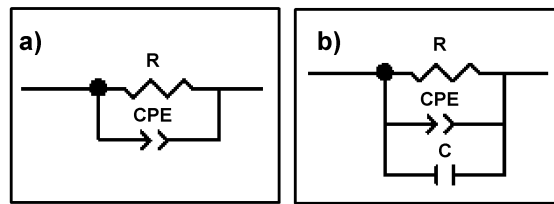


Figure 2. Equivalent electrical circuits used to model the data.

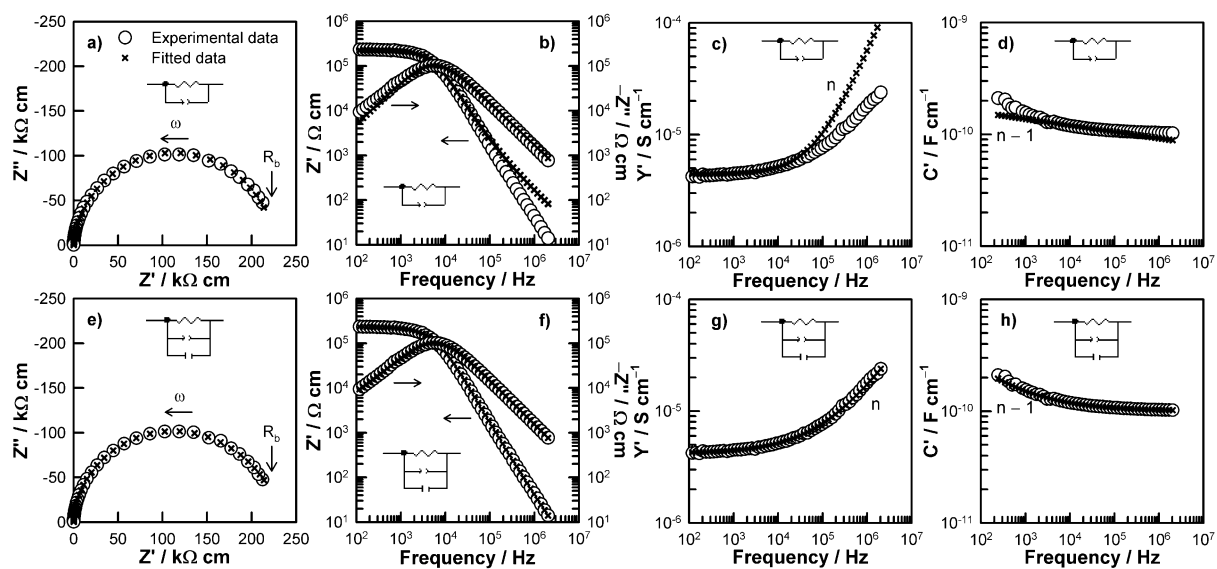


Figure 3. BT_2 : impedance complex plane plots (a,e) and spectroscopic plots of Z^* (b,f), Y' (c,g) and C' (d,h).

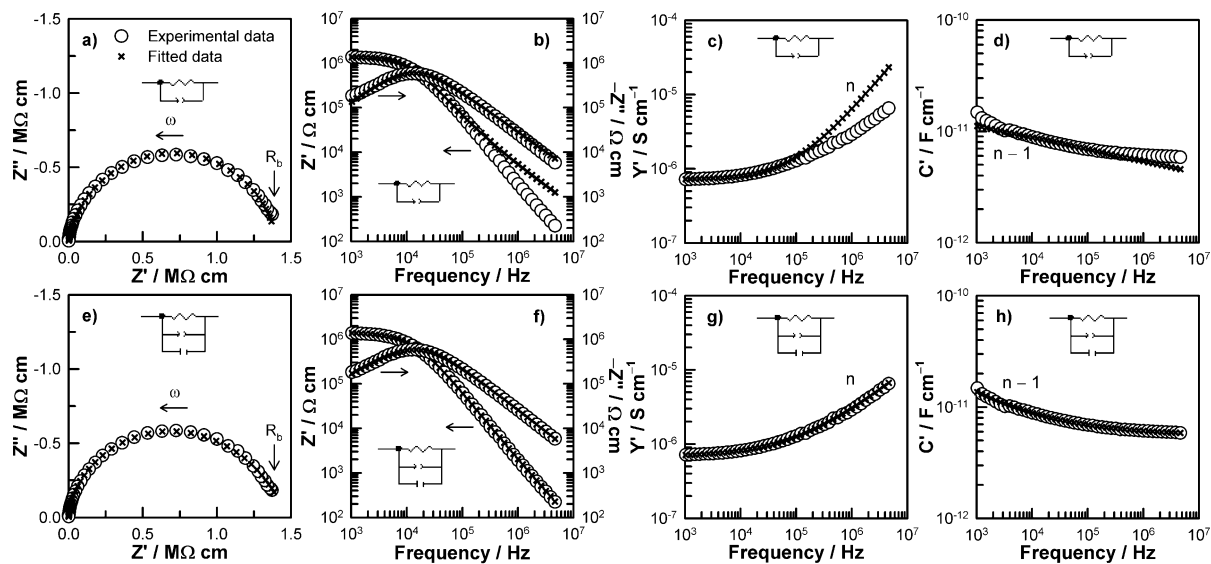


Figure 4. YSZ: impedance complex plane plots (a,e) and spectroscopic plots of Z^* (b,f), Y' (c,g) and C' (d,h).